Thermal Decomposition of TATB—Review of Molecular Characterization

Evan M. Kahl and John G. Reynolds

Lawrence Livermore National Laboratory
Livermore CA 94550

ABSTRACT

The behavior of TATB when exposed to thermal insults is important to understand on a molecular level when developing safety response procedures. This manuscript summaries the current state of studies on the thermal decomposition of TATB and subsequent decomposition products.

INTRODUCTION

TATB (1,3,5-triamino-2,4,6-trinitro-benzene) is a fascinating molecule to study from a fundamental to applied perspective. The molecule was first prepared in 1888 [1] by Jackson and Wing, and since that time has been the subject of many studies because of the unique structural configuration. From a fundamental perspective, the full substitution around the benzene ring with alternating donor-acceptor groups yields interesting reactive properties. The crystalline structure [2] shows the organization of the lattice has a similar appearance to two-dimensional sheets of graphite instead of a tertiary structure expected from an organic compound with numerous heteroatoms. The donor-acceptor configuration has been also studied from a computational aspect [3] showing an unusual electron density distribution straining the bonding of benzene ring. These molecular features apparently lead to a stability that makes TATB only slightly soluble even in the more robust organic solvents, such as DMSO and HMPA [4] and shows an relatively inert [5] to reactivity. From the applied view, TATB has extensively used as an insensitive explosive. The unusual overall structure makes it resilient to insults such as impact, friction and spark, as well as the reasonably robust thermal properties make it a thermally stable compared to other military munitions [6]. The unusual properties are also reflected in the non-linear optics applications [7] where the non-dipolar molecule should not have the strong second-generation harmonic needed for the optical properties that it displays. These features have gleaned more than a pedestrian interest in this unusual molecule.

The use of TATB as a munition has stimulated interest in determining the origin and extent of the unusual stability. The principal drivers for this are the potential extreme conditions the explosive is exposed to as a munition. Conditions such as extreme temperature changes, radiation and impact have the potential to alter the chemical and physical properties of TATB. These types of changes can affect the performance properties as well alter protocols for safe handling and storage. Of particular interest is the thermal stability, which studies have yielded many efforts to understand and model the thermal degradation pathways of TATB. This manuscript reviews the published background into the thermal reaction pathways of TATB and TATB related materials, such as polymer bonded explosives, and reviews the efforts to characterize the decomposition products on a molecular level.

SUMMARY OF TATB THERMAL DECOMPOSITION PATHWAYS

The bulk of the research into the thermal decomposition behavior of TATB has occurred in the last fifty years. Early work concentrated on determining global kinetics and activation energies of thermally initiated reactions. This work gradually led to efforts to characterize molecular species. From this perspective, Figure 1 summarizes some of the major species identified in this decomposition route. Currently, benzo-furazans (or furazans used here), TATB-F_1, -F_2, and -F_3, are considered to be the main components in the first steps of decomposition. Benzo-furoxans (or furoxans used here), TATB-F_{x1}, F_{x2}, and F_{x3}, are still being considered, but probably play an important part in non-thermal decomposition processes, such as irradiation and impact.

During the thermal process, after formation from TATB, these compounds begin to unravel, probably first losing the appendages of the aromatic ring followed by cleavage of the ring. This leads to many potential molecular compounds of various structures that contain ring fragments and lead to the formation of light gases. Table 1 summarizes essentially all the molecular species detected as ions in mass spectrometry (MS) studies of thermal decomposition of TATB. Towards the end of the decomposition process, after most the functionality has disappeared, a carbonaceous residue is formed. This residue appears to have very loose structure and may have some integration of C-N structures into the carbon framework.

X-ray photoelectron spectroscopy (XPS) and MS data with supporting infrared spectroscopy (IR) and Raman data provides the bulk of the evidence that leads to identifying the furazans and other products. MS and IR have also been

critical in the light gas analysis. The studies that provide these data and formulate potential structures on the molecular level that support the decomposition scheme in Figure 1 and the species in Table 1 are discussed in detail below.

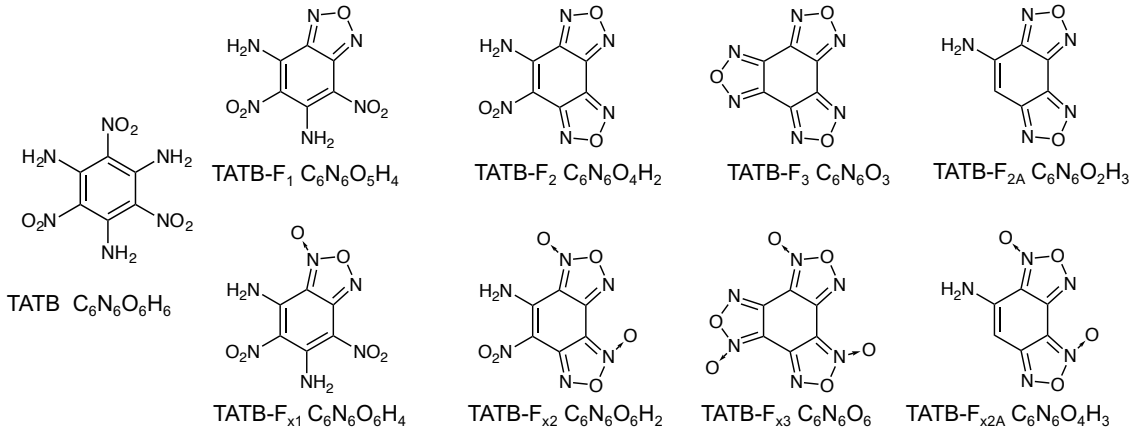

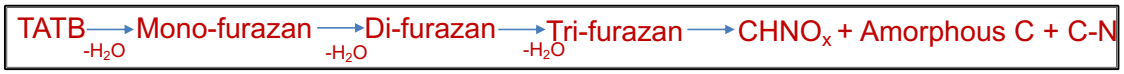

Figure 1. Summary of the conceptualization of TATB decomposition pathways

Table 1. Summary of detected ion from mass spectrometric studies on TATB thermal decomposition

m/z	Possible ions	m/z	Possible ions	m/z	Possible ions	m/z	Possible ions
16	O, CH_4	46	NO_2	104	Multiple Ions	176	Unidentified
17	OH, NH_3	52	C_2N_2	110	$C_4N_2O_2H_2$	177	Unidentified
18	H_2O	58	$(CH_3)_2C=O$	114	$C_3N_3O_2H_3$	182	$C_6N_4O_3H_6$
26	CN	68	C_2N_2O	119	$C_6N_2OH_3$	204	$C_6N_6O_3$
27	HCN	70	C_2NO_2	120	C_4N_4O	222	$C_6N_6O_4H_2$
28	CO, N_2	80	Multiple Ions	128	$C_3N_2O_4$	224	$C_6N_6O_4H_4$
30	NO	86	$C_3N_2O_2H_2$	131	Multiple Ions	228	$C_6N_5O_5H_6$
40	Ar, C_2NH_2	92	C_7H_8	144	$C_3N_3O_4H_2$	229	Unidentified
43	HNCO	96	$C_4N_2OH_2$	147	$C_6N_4OH_3$	241	$C_6N_6O_5H_5$
44	CO_2, N_2O	98	$C_3N_2O_2H_2$	165	$C_6N_4O_2H_5$	258	TATB

Regardless of the plethora of research into this topic, there remains many unanswered and unsubstantiated claims into the effects of thermal exposure on TATB. Given the importance of this topic to the energetic materials community, these claims need to be verified and a comprehensive decomposition mechanism(s) must be developed to be applied for predictive purposes in case of thermal accidental scenarios.

CHARACTERIZATION OF DECOMPOSITION PRODUCTS

When TATB is heated, the decomposition produces gases and solids. The amount of gas and solid depend on the severity of the thermal conditions—temperature, time of exposure and confinement. Confinement in these studies refers to a closed system that does not readily vent but usually does not have added pressure, so the pressure builds according to the decomposition until the system fails to hold pressure. When TATB is heated in a closed system, if the conditions are right, it will eventually produce enough volatile gases, so the system will rupture the confinement. TATB is generally not used in the pure form in munitions, so some studies have included polymer bonded explosive mixtures. TATB is usually the 90+% component of these mixtures, so the thermal decomposition studies are dominated by the behavior of TATB.

Farber & Srivastava. Efforts to identify molecular intermediates in the thermal decomposition of TATB commenced in the latter half of the 20th century. Farber & Srivastava [8] applied MS to analyze volatile species evolving from TATB when thermally heated. The work attempted to distinguish a spectral signature of TATB from thermal degradation products by using different size openings in the cells that held a small sample of TATB in a reaction

chamber. To promote only detection of the parent ion of TATB, a Langmuir cell under vacuum was heated around the reported sublimation temperature of TATB. To promote fragmentation during thermal events, a modified Knudsen effusion cell was used while heating in the thermal reaction regime, 200 to 300 °C. The modified Knudsen cell was designed to specifically cause intra-cell collisions. Formed species were monitored using MS. The electron impact ionization source was tuned to minimize the production of m/z 212 ion, TATB minus -NO_2 from the m/z 258 ion, to minimize fragmentation.

ion	TATB	Thermal
258 ($C_6N_6O_6H_6$)	84	
144 ($C_3N_3O_4H_2$)	7	65
128 ($C_3N_2O_4$)	20	80
114 ($C_3N_3O_2H_4$)	7	100
98 ($C_3N_2O_2H_2$)	25	60
86 ($C_2N_2O_2H_2$)	7	35
70 (C_2NO_2?)		60
46 (NO_2)		33
44 (CO_2)		48
30 (NO)		30
28 (CO, N_2)		70
18 (H_2O)		25
2 (H_2)		4

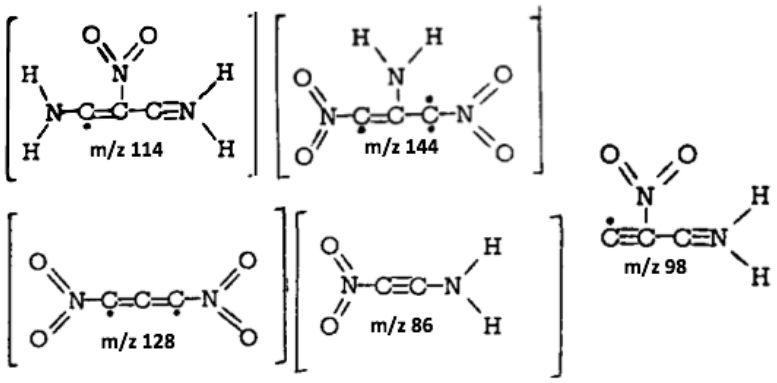

***Figure 2**. MS ions identified for TATB, TATB fragments and fragments of thermal products from the heating of TATB in a Langmuir cell and a modified Knudsen cell from Farber & Srivastava [8]*

Figure 2, left side, shows some potential structures of these ions produced at 250 °C. The column marked TATB shows relative ion intensities detected from the direct evaporation Langmuir cell, while the column marked Thermal is relative ion intensities detected from the Knudsen effusion cell. In the Langmuir experiment, the parent TATB was clearly observed, but there also was some fragmentation or thermal decomposition, but no light gases. In the effusion experiment in the Knudsen cell, there was no parent ion, but intense ions from fragments or thermal decomposition products, including light gases. Products from both cells show fragments that necessitate the cleavage of the aromatic ring. Figure 2, right side, shows some suggested structures from the study of products. Prominent ions that contain N, C, and O from the Knudsen cell are m/z 144, 128, 114, and 98. These are also observed in the TATB fragmentation, but of much less relative intensity. The light gases are considered evidence of thermal reaction. Only the product from the effusion cell show several low molecular weight light gases, such as CO_2 and NO_2. Furazans and furoxans were not detected. Appearance of the TATB parent ion with the m/z 144, 128, and 114 was suggested as a way to discern TATB fragmentation from TATB thermal degradation, but no unequivocal link was made indicating the TATB or thermal degradation products could be discerned by identification of these ions. However, suggestions were made on how the cleavage to produce these species is consistent with the molecular structure of TATB, based on bond lengths from the original crystal structure. Also, based on m/z 114 ion behavior at different temperatures, an activation energy was calculated to be 179.9 kJ/mol (43 kcal/mol).

Catalano & Rolon. Catalano & Rolon [9] studied the isothermal decomposition of TATB at selected temperatures in the range of 200 to 312 °C under confinement using IR, MS, and pressure-time response for product gas analyses. The samples were generated in an assembly that could be immersed in a constant temperature bath. The gaseous products were sampled through an on-line manifold; pressure was maintained at 10 ksi. As the pressure increased to over 10 ksi, a pressure reduction value would open, and a sample was collected. The valve would close again when the sample pressure was below 10000 psi. The products were then analyzed by matrix isolation IR on a cooled CsI window, or by MS of batch-collected gas. The gaseous evolution behavior was grouped into endothermic, exothermic and explosion based on the behavior of gas evolution when heating was terminated. Samples that did not continue to produce pressure upon removal from the heat source were considered endothermic; samples that did continue to generate pressure were considered to be exothermic; and samples that ruptured the seal were considered an explosion. Table 2 shows a summary of gases generated over the entire isothermal study. Some findings that provide product decomposition insight are: CO_2, H_2, and H_2O were observed at all temperatures, CO_2 and H_2O were only detected in endothermic samples; NO, N_2O, and NO_2 were detected in notable quantities only in exothermic samples; CO_2/H_2O concentration ratio could not be correlated to reaction conditions; C_2N_2 and HCN were only observed in explosion samples. Acetone, m/z 58, was considered residual solvent from the synthesis process and not a light gas from decomposition.

The conclusions from these experiments began to clarify the thermal decomposition mechanism of TATB. The low temperature evolution of H_2O, N_2, and CO_2, and acetone in the endothermic stage was presumed to be intercalated. No accounting of the release of H_2 was made in the endothermic stage, but in the exothermic stages, the amounts of

CO_2, H_2O, N_2, and H_2 released were too large to be accounted for by intercalation, and that intramolecular water abstraction cannot be an important mechanism because so little water is produced. Note: furazans and furoxans were not mentioned in this study.

***Table 2**. Gas-phase MS ions identified in isothermal decomposition studies of TATB from 202 to 312 °C; numbers in parentheses are m/z of ions; from Catalano & Rolon [9]*

Intensity of Species	Endothermic	Exothermic	Thermal explosion
Major	CO_2 (44)	CO_2 (44)	CO_2 (44)
Major	H_2O (18)	N_2 (28)	CO (28)
Major	N_2 (28)	H_2O (18)	HCN (27)
Major	$(CH_3)_2CO$ (58)		N_2 (28)
Middle			NO (30)
Minor	CO (28)	CO (28)	C_2N_2 (52)
Minor	N_2O (44)	N_2O (44)	H_2 (2)
Minor	NO (30)	NO (30)	H_2O (18)
Minor	H_2 (2)	H_2 (2)	
Minor	CH_4 (16)	CH_4 (16)	

In a follow-up study, Catalano & Rolon [9] examined the solid-state residues from the confined reactions described above to characterize degradation of molecular species in final products. They also compared those results to solid residues from select unconfined thermal experiments. In product residues (from confined) and condensates (ODTX experiments), isolated solid phases primarily exhibited TATB with trace levels of unknown, but similar to TATB, structures. The residues from unconfined experiments yielded distinctly different structural configuration than the confined residues based on IR, optical and SEM results. Crystal morphologies were identified in most samples whether confined or unconfined, but these morphologies exhibited some differences. Molecular structures in these materials were not identified, but a reaction sequence was developed based on these observations as a function of treatment temperature. Broadening of IR features support multiple species in these residues.

Notable conclusions about thermal decomposition of TATB from this study were: unconfined decomposition is different than confined decomposition; no intermediates were detected in the residues obtained from the confined decompositions, just slight variations on TATB structure; possible other morphologies of TATB crystals were either formed or highlighted by confined decomposition; unconfined decomposition yielded a sequential TATB decomposition pathway, TATB $\rightarrow A_{T = 573\ K} \rightarrow B_{T = 619\ K} \rightarrow C_{T = 624\ K}$ (any product representing a multitude of species); H_2O abstraction is not important; no evidence of furazan production (probably). Two points worth stressing are the IR behavior of unconfined residues in the 3000 cm^{-1} to 3500 cm^{-1} range appeared quite broad (*vide infra*), and the appearance of a sharp feature around 2200 cm^{-1} which was not identified in the study but could be assigned to C-N bonding in the unconfined residues (does not appear in the confined residues; just low intensity -NH_2 and -NO_2 features of TATB).

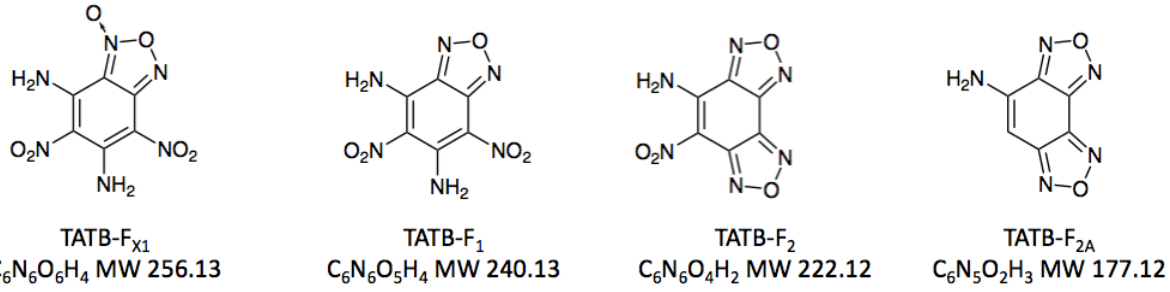

***Figure 3**. Compounds identified by MS in the decomposition of TATB by a) electron irradiation (first three from the left) and b) shock and thermal treatment (first three from the right) Sharma et al. [10]*

Sharma et al. Sharma et al. [10] studied TATB decomposed by shock, irradiation and thermal exposure using XPS with other supporting spectroscopies. The original experiments were performed using a small impact cell to expose the TATB to shock and *in-situ* stimulation to expose the TATB to irradiation. The primary identification was through the behavior of the N1s XPS spectra exhibiting some changes in the -NO_2 and -NH_2 nitrogen features. Follow-up experiments focused again on the N1s XPS spectra supported by the C1s, O1s, valence band and Auger spectra.

Furazans and furoxans as decomposition products were potentially identified in samples exposed to UV and electron beam irradiation, impact, and thermal treatment.

Figure 3 shows four decomposition products of the treatment of TATB that were detected and identified by thin layer chromatography (TLC) coupled to MS and verified in residues by XPS. The products were extracted from the residues with acetone (CH_3COCH_3). The first three structures were observed in electron beam irradiated samples. The last three structures were identified in the thermally treated residues. The XPS N1s shows broadening of the feature assigned to amino-N and a shift in the feature assigned as the nitro-N to a lower binding energy. These features were attributed to the appearance of furoxans and furazans.

Subsequent samples prepared by various methods, such as shock and impact under water provided further evidence of the furazan- and furoxan-type species in the reaction products. Low levels of furoxans were observed in the shock samples but a mixture of furoxans and furazans were observed in the impact samples isolated from acetone extracts. Assignments of position and behavior of the N1s XPS spectra were fortified by model compounds related to the benzo-furoxans and benzo-furazans, as well as TLC and MS.

Conclusions about thermal decomposition of TATB from this work were: 1) two H and one O were lost, 2) the products are chemically changed from TATB, 3) H_2O is formed and is exothermically similar to derived activation energy. Chronologically, this is the first time in the literature that benzo-furazans (TATB-F_1, -F_2) and benzo-furoxan (TATB-F_{X1}) were identified as products of damaged TATB. Note that the furoxan is only detected from non-thermal decomposition conditions, while the furazans are detected from most thermal decomposition conditions. The bulk of the evidence for these species existing in the reaction products comes from studies presenting several XPS results [10]. It is important to note, as far as the peer review literature indicates, the MS data supporting these structures was not presented in these publications, and that validation of these structures is only casual.

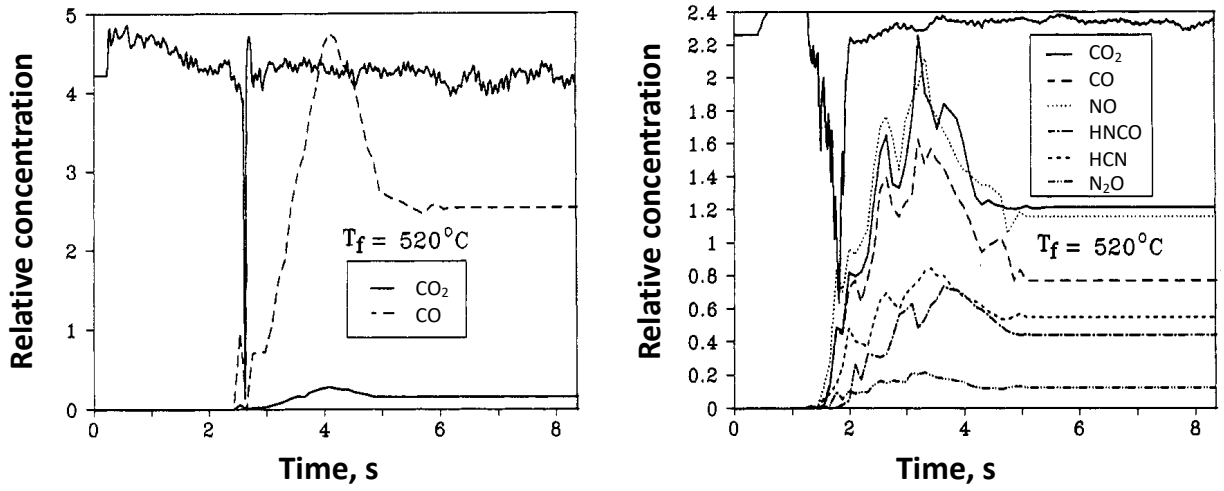

Figure 4. *T-Jump/FTIR data for (left side) trinitro-benzene heated at 2000 °C/s to 520 °C under 40 atm Ar; control voltage shows sharp exotherm (pointing down) at approx. 2.5 s; (right side) TATB heated at 2000 °C/s to 520 °C under 10 atm Ar; control voltage exotherm has minimum at approx. 1.9 s from Brill & James [11]*

Brill & James. Brill & James [11] conducted a series of rapid heating experiments to discern mechanisms caused by shock and impact of TATB (and other nitro-substituted benzenes. Using the T-jump, rapidly heating from RT to 422 °C in 20-500 μs (2000 °C/s to constant temperatures of 500 °C or higher), the concentrations of several volatile gases, CO_2, CO, NO, HCN, HNCO, and N_2O were monitored by FTIR. Figure 4 (left) compares the thermal reaction behavior of trinitro-benzene (TNB). The TNB exhibits are sharp exotherm indicating a narrow reaction barrier and only CO_2 and CO evolving. H_2O evolved but was not quantitated. Figure 4 (right) exhibits the same experiment for TATB. In this case, the exotherm is broad and jagged indicating several reactions were occurring. As well, the products were a wider range of light gases, indicating different reaction mechanisms than TNB probably because of involvement of the amino groups during decomposition. H_2O evolved but was not quantitated. Note the formation of the light gas, HNCO. This had not been seen in previous reports on light gases. Also, the report highlights that the total heat from the exothermic products (CO, CO_2, HNCO) decreases and that from the endothermic products (NO, N_2O, HCN) increases when NH_2 groups are present.

Land et al. Land et al. [12] reported a comprehensive MS study that provides more information on higher molecular weight species evolving during thermal decomposition, but also includes lighter gases. The MS detection was

by a rare method, STMBMS (simultaneous thermogravimetric modulated beam MS with time-of-flight detection). This study included parent ion detection, thermal degradation, and deuterium isotopic labeling. The TATB identification experiments utilized a lower temperature, around 250 °C, and a cell with a larger orifice to reduce intermolecular collisions. The thermal decomposition was promoted by heating the TATB at a higher temperature in a cell with a smaller orifice to promote intermolecular collisions. The isotopically labeled experiments were performed in the same manner. The deuterium label replaces the hydrogen atoms on the N atoms of the amino groups (-NH_2 converted to -ND_2).

***Table 3**. Gas-phase MS ions identified for analyses of TATB and corresponding deuterated TATB listing parent and fragment ions and suggested formulas from Land et al. [12]*

Ion	Fraction	TATB-d_6	Formula
258	47%	264	$C_6N_6O_6H_6$
241	1%	246	$C_6N_6O_5H_5$
229	1%		
228	15%	234	$C_6N_5O_5H_6$
224	3%	228	$C_6N_6O_4H_4$
182	2%	188	$C_6N_4O_3H_6$
165	2%	170	$C_6N_4O_2H_5$
147	1%	150	$C_6N_4OH_3$
120	1%	121 or 124	
119	2%	122	$C_6N_2OH_3$

Table 3 shows the ion mass, fractional intensity, deuterated ion mass and suggested formula at the conditions designed to minimize side reactions, accentuating TATB detection without thermal decomposition. The TATB parent ion, m/z 258 is the major ion detected. The TATB-d_6 parent ion, m/z 264, confirms the deuterium is on the -NH_2 groups. This also matches the results of the Langmuir cell experiment by Farber & Srivastava [8] above, where the parent ion is the prominent ion for TATB. The ion at m/z 241 is assigned a formula that is could be TATB-F_1 + H. Likewise, other ions could be identified as TATB-F_2 + 2H. Ions that could be identified as TATB-F_3 do not appear. This may have been a result of the ionization dynamics of the cell chosen for the volatilizing the TATB. The balance of the ions in the table are assigned as MS fragments that have the aromatic ring intact (C_6 with substitutions). Although there are some overlaps with assignments of ions as in the Langmuir experiments most of the ions detected are not the same. In the Langmuir case, the fragments to be formed from cleavage of the aromatic ring. In this study, all the fragment ions are in low relative concentration except for m/z 228. This was assigned to a species that has a N atom missing.

***Table 4**. Gas-phase MS ions identified for analyses of thermally treated TATB and corresponding deuterated TATB listing parent and fragment ions and suggested formulas from Land et al. [12]*

Ion	Fraction	TATB-d_6	Formula	Ion	Fraction	TATB-d_6	Formula
240	4%	244	$C_6N_6O_5H_4$	52	7%	52	C_2N_2
222	4%	224	$C_6N_6O_4H_2$	44	16%	44	CO_2
204	1%	204	$C_6N_6O_3$	43	8%	44	HNCO
177	2%			30	20%	30	NO
176	1%			27	8%	28	HCN
164	2%			18	14%	20	H_2O
120	2%	120	C_4N_4O	17	2%	20	NH_3
68	1%	68	C_2N_2O				

Table 4 shows the STMBMS investigation of the thermally treated products of TATB and TATB-d_6, showing the m/z of the ions, the relative intensities, and suggested formulas. The first three entries are the furazans, TATB-F_1, -F_2, -F_3. Below these are several ions that are considered fragments from these intermediates. The ion at m/z 177 has been observed before and has been assigned in the shock study to be TATB-F_{2A}, by Sharma et al. [9]. Ions with m/z values lower than this have been assigned to fragments where the aromatic ring has been cleaved in some manner. Light gases are detected as m/z 44 or smaller. *Notable is that none of the ions in Table 4 agree with the ions in Table 3*. The distinction is that the parent TATB is represented by fragment ions that are different than products or the fragment ions of the products from thermal reactions. In addition, without actual data, it is hard to unequivocally

show that the thermal decomposition products from this study agree with those of shock studies, but, the light gas data appears to be essentially the same as found generally in the isothermal DSC of Catalano & Rolon [9] and the Knudsen effusion study of Farber & Srivastava [8].

Significant conclusions came from this study were: furazans were detected in thermal decomposition products; ions produced from conditions designed not decompose the TATB were different than those produced from conditions designed to decompose TATB; light gases were in agreement with previously published studies on TATB thermal decomposition.

Makashir & Kurian. Makashir & Kurian [13] monitored the isothermal decomposition of TATB in a specially fabricated high temperature IR cell with isothermal temperature control. Spectra were recorded on KBr discs at selected reaction times. The variation in intensity of the -NO_2 symmetrical stretching vibration at 1220 cm^{-1} was used to quantitate the changing concentration of the TATB.

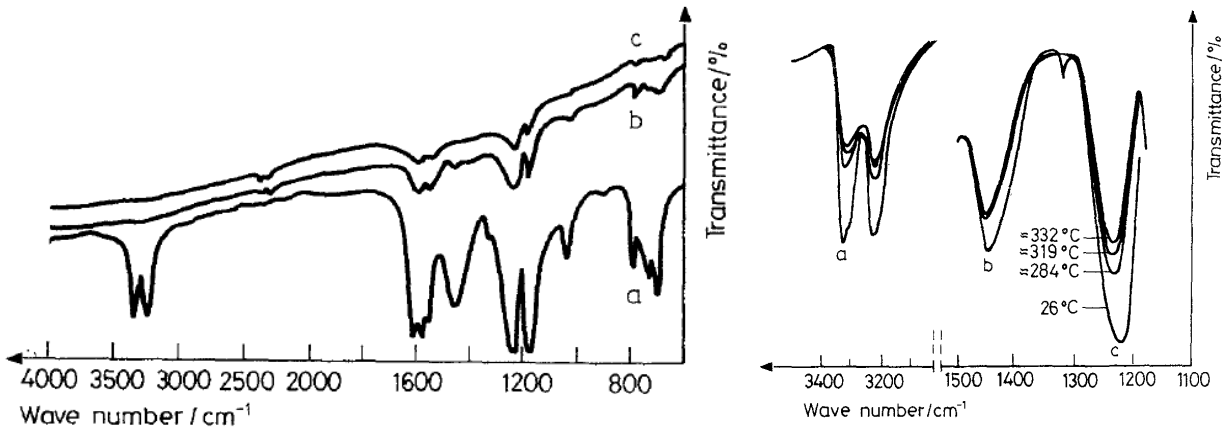

Figure 5. *IR spectra (left side) TATB at a) 25 °C, b) 294 °C after 13 min, c) 294 °C after 45 min; (right side) variation in diagnostic IR vibrations at selected temperatures a) 3320 cm^{-1} (-NH_2 asymmetric stretching), b) 1440 cm^{-1} (ring stretching), c) 1220 cm^{-1} (-NO_2 symmetric stretching) from Makashir & Kurian [13]*

Figure 5 (left side) shows IR spectra of the temporal behavior of TATB heated in the special cell at 294 °C. The a) spectrum shows the starting TATB before thermal degradation. This spectrum is typical of TATB and the regions between 3000 cm^{-1} and 3500 cm^{-1} 1000 cm^{-1} to 1600 cm^{-1} show diagnostic features that include -NH_2, -NO_2, and ring IR modes. As the heating progresses, many of these features diminish indicating the residual material is losing these functionalities. The spectrum at 45 min shows that most of these features are absent in the residual material. Note also the low intensity features between 2000 cm^{-1} and 2500 cm^{-1}. These features were reported to develop as the decomposition progressed and were assigned to species that have C-N, C-C, and C-O conjugated in the decomposition products. However, these features then disappeared at high temperatures. Figure 5 (right side) shows the behavior of several of these diagnostic bands as a function hold temperature. As the temperature of treatment increases, these diagnostic features decrease in intensity, supporting the loss of substitution on the ring as well as ring changes during decomposition.

Some interesting conclusions from this study were that the intensity of the -NH_2 stretching vibration disappeared faster than the -NO_2 symmetric stretching vibration which disappeared faster than the ring stretch, suggesting an order of reactivity—amino group > nitro group > ring. Interesting that Sharma et al. [10] stated the nitro group reacted faster than the amino group. Regardless, these observations support the concept of that the ring substituents react before the ring falls apart, as observed in the Faber & Srivastava [8] and Land et al. [12] results (*vide supra*). Also, in the residue analysis, evidence of C-N and other condensed species was reported at least as intermediates to the formation of the final products.

Belmas et al. In a series of papers, Belmas et al. [14] studied the results of T2 (French version of polymer bonded TATB) subjected to isothermal TGA at temperatures 200 to 330 °C. The product gases and solids were examined for thermal decomposition products. The light gases produced during the isothermal experiments were analyzed by GC-MS and the results were only presented as a mass balanced equation, assuming all the experimental data at different isothermal conditions were used. Table 5 shows this distribution. The solids were extracted using acetonitrile and analyzed using HPLC. Structures of the solid-phase extractants were verified by pure compounds. Overall kinetic behavior of T2 determined by TGA was compared to model compound decomposition and was analyzed using a simple kinetic model. TATB-F_1 and TATB-F_2 were detected during the decomposition and verified by comparisons to pure compounds.

The species detected in this study overlap with the results of the isothermal study by Catalano & Rolon shown in Table 2 . In that study, CO and CH_4 were also detected, but the difference is probably a MS detection issue due to the overlapping m/z values of these species. The isothermal study detected m/z 44, N_2O, not listed in Table 5 and m/z 52 only during thermal explosion. Note that N_2O cannot be distinguished from CO_2 by MS alone. In the Knudsen experiment by Faber & Srivastava, shown in Figure 2, the same masses were identified. In addition, m/z 46, NO_2, was also identified. In the STMBMS study by Land et al., m/z 43, HNCO, and m/z 68, C_2N_2O, were also observed, but not seen in this T2 study. Brill & James in the T-Jump experiments observed HNCO also.

Table 5*. Gas-phase MS ions identified from analyses of thermally treated T2 (polymer-bonded TATB) at isothermal conditions, moles of gas produced with respect to 1 mole TATB from Belmas et al. [14]*

Gas	H_2O	HCN	N_2	NO	CO_2	C_2N_2
m/z	18	27	28	30	44	52
moles	2	0.48	0.4	0.96	1.14	0.91

Some interesting conclusions from this series of studies were: 1) mono-benzo-furazan and di-benzo-furazan were detected, but tri-benzo-furazan was not; 2) furazans quickly vanished as soon as generated (explained by a lower decomposition temperatures than TATB); 3) combined gas composition and furazan quantitation validated the proposed mechanism of TATB by Land et al. [12] TATB $\rightarrow$ mono-benzo-furazan + H_2O $\rightarrow$ di-benzo-furazan + H_2O $\rightarrow$ to gases + solid residue; 4) stoichiometry of decomposition of TATB is 0.4 N_2 + 0.96 NO + 1.14 CO_2 + 2.0 H_2O + 0.91 C_2N_2 + 0.48 HCN.

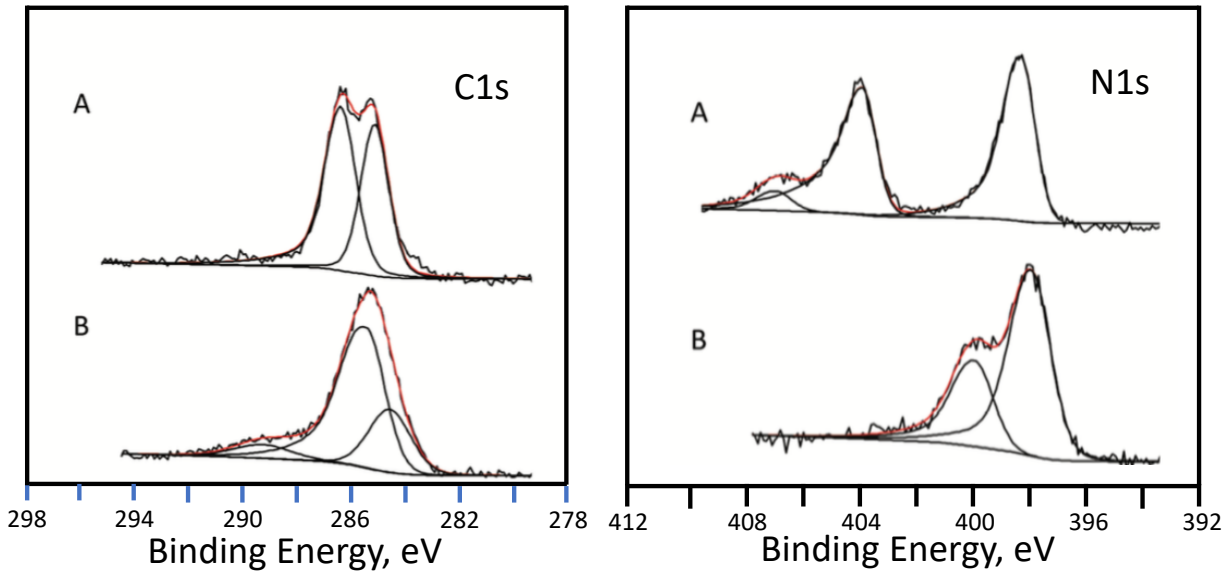

Figure 6. XPS spectra of ultra-fine TATB (A) and pyrolyzed product (B): left side C1s and right side N1s taken from Carter et al. [15]

Carter et al. Carter et al. [15] studied characterized products from shock compressed TATB by XPS, IR, and Raman spectroscopy. As a supporting effort, pyrolysis samples generated by heating ultra-fine TATB powder in an open Pt crucible at 400 °C in dry N_2 for 35 min were also studied. The black powder residue exhibited several spectroscopic features relevant to thermal product characterization. Figure 6 shows the XPS spectra of TATB and the pyrolyzed sample.

The C1s spectra for the TATB matches closely to the XPS of previously published data of Sharma et al. [8]. Two partially resolved maxima are assigned through fitting to be due to C-NH_2 (286.4 eV) band C-NO_2 (285.1 eV). The N1s spectra exhibits two well separated maxima that have been assigned to -NH_2 (398 eV), -NO_2 (404.0 eV) and a satellite at 407.0 eV.

Thermal degradation clearly changes the structure of the material. Quantitative analysis indicated the sample is primarily carbon and nitrogen with a little oxygen (atomic concentrations: TATB—$C_{0.33}N_{0.33}O_{0.33}$; pyrolyzed product $C_{0.67}N_{0.34}O_{0.02}$). The C1s spectrum of the pyrolyzed product appears as a broad unresolved maximum. Based on peak shape analysis, the peak is likely a multitude of different species and can be fit to several maxima. For simplicity, only three components were shown and assigned as sp^2 C-C (284.4 eV), sp^2 C-N (285.4 eV) and R-COOH (289.4 eV).

The appearance of the carboxylic acid functionality could have been from surface oxidation occurring during handling. The N1s spectrum of the pyrolyzed product exhibits a broad feature with a higher eV shoulder. This was deconvoluted and assigned to R-NH_2 (398.1 eV), N_5 C-N (400.1 eV). The R-NH_2 functionality was assigned based on the similarity of with the R-NH_2 feature in the TATB spectrum as well as Raman and IR data also taken on these samples. The IR data of the pyrolyzed product is significantly different than the IR of TATB exhibiting features that are much more like carbon-nitride thin films. Many spectroscopic studies, XPS, IR, nuclear magnetic resonance (NMR) and others, have been performed on these types of material and the N1s C-N feature of the pyrolyzed spectrum is similar, appearing as N fully incorporated into the carbon network. These types of nitrogen are N-5, N-6, or N-Q, where the N-5 or N-6 nitrogen occupies an edge site of a sp^2 carbon sheet as a heteroatom within a 5- or 6- membered ring. Suggested with comparison to thin film literature, the N is likely found as N in a five membered ring, and an N-Q nitrogen populates an interior site of the carbon sheet with three carbon−nitrogen bonds.

Some relevant conclusions from this study were: Sharma et al. [10] assignments of the XPS spectra were basically correct although this study provided better resolved data; thermal degradation essentially leads to destruction of TATB forming polymerized carbon with C-N possibly incorporated into the structure.

CONCLUSIONS

Some of the highlights of these studies on thermal decomposition of TATB are: *Farber & Srivastava* established thermal treatment produces ring cleavage and light gases but also products that still contain heteroatoms. *Catalano & Rolon* validated the gas evolution and established the types of gases evolving from the thermal decomposition of TATB reflected the severity of the heating. They also established treatment in unconfined conditions leads to a complicated decomposition pathway while the confined condition does not reveal intermediates. *Sharma et al.* established the existence of decomposition products with functionality from amino and nitro groups condensing. They also established the structure of these groups reflects the type of insult, such as thermal, impact or irradiation. *Brill & James* established the thermal decomposition under confinement is a complicated series of reactions compared to non-amino containing explosives. *Land et al.* validated the existence of furazans and other products from ring cleavage. They also did not observe furoxans in the thermal products. *Makashir & Kurian* showed the functionality on TATB vanishes on the path to final residue. They also observed the possibility of heteroatom inclusion in the final product. Belmas et al. provided identification of furazans by synthesis of pure compounds and validated the furazan decomposition pathway. *Carter et al.* substantiated furazans as products as well as C-N incorporation into final residues.

Substantial progress has been made in the identification of molecular species that are part of the thermal decomposition pathways of TATB. However, much more needs to be done to cement a comprehensive decomposition network. Some ideas towards this goal are: establishing kinetics for production and destruction of major species; unequivocal identification through comparison to pure compound behavior; more complete characterization of residues; *in-situ* decomposition monitoring.

Acknowledgment

This work was performed under the auspices of the U.S. Department of Energy by Lawrence Livermore National Laboratory under Contract DE-AC52-07NA27344. LLNL-PROC-755282 (941913).

References

[1] C. L. Jackson and J. F. Wing, "On Tribromotrinitrobenzol," *Proceedings of the American Academy of Arts and Sciences*, 23 (1), 138-148 (1887); C. L. Jackson and J. F. Wing, "On benzo-tri-sulfonic acid," J. Am. Chem. Soc. 9, 324-355 (1887); C. L. Jackson and J. F. Wing, "On Tribromotrinitrobenzol," J. Am. Chem. Soc. 10, 283-294 (1888).

[2] H. H. Cady and A. C. Larson, "The Crystal Structure of 1,3,5-triamino-2,4,6-trinitro benzene, *Acta Crys*t., 18, 485-496 (1965).

[3] R. H. Gee, S. Roszac, K. Balasubramanian, and L. E. Fried, "Ab Initio based Force Field and Molecular Dynamics Simulation of Crystalline TATB," *J. Chem. Phys*., 120, 7059-7066 (2004).

[4] W. Selig, "Estimations of the Solubility of 1,3,5-triamino-2,4,6-trinitro benzene (TATB) in various solvents," Lawrence Livermore National Laboratory report UCID-17412, March 2, 1977; M. F. Foltz, D. L. Ornellas, P. F. Pagoria and A. R. Mitchell, "Recrystallization and Solubility of 1,3,5-triamino-2,4,6-trinitrobenzene in dimethyl sulfoxide," *J. Mater. Sci*., 31, 1893-1901 (1996).

[5] P. C. Hsu, C. J. Souers, M. DeHaven, R. Garza, J. Alvarez, and J. E. Maienschein, "Characterization of Thermally Damaged LX-17," *Journal Thermal Analysis and Calorimetry*, 93 (1), 311-317 (2008).

[6] B. M. Dobratz, "The Insensitive High Explosive Triaminotrinitrobenzene (TATB): development and characterization-1888 to 1994," report LA-13024H, Los Alamos: National Laboratory; August 1994.

[7] I. G. Voight-Martin, G. Li, A. K. Yakaminaski, J. J. Wolff, and H. Gross, "Use of electron Diffraction and High-Resolution Imaging to Explain why the Non-dipolar 1,3,5-triamino-2,4,6-trinitro benzene Displays Strong Powder Second Harmonic Generation Efficiency," *J. Chem. Phys. A*, 101, 7265-7276 (1997).

[8] M. Farber and R. D. Srivastava, "Thermal Decomposition of 1,3,5 triamino-2,4,6-trinitrobenzene," *Combustion and Flame* **42**, 165-171 (1981).

[9] E. Catalano and C. E. Rolon, "A Study of the Thermal Decomposition of Confined Triaminotrinitrobenzene. The Gaseous Products and Kinetics of Evolution," *Thermochim. Acta*. **61**, 37–51 (1983), doi:10.1016/0040-6031(83)80302-5; E. Catalano and C. E. Rolon, "On the Solid-State Products of the Thermal Decomposition of Confined and Unconfined Triaminotrinitrobenzene," *Thermochimica Acta*, **61**, 53-71 (1983).

[10] J. Sharma and F. J. Owens, "XPS Study of UV and Shock Decomposed Triamino-trinitrobenzene, *Chem. Phys. Let.* **61** (2), 280-282 (1979); J. Sharma, W. L. Garrett, F. J. Owen, and V. L. Vogel, "X-ray Photoelectron Study of Electronic Structure and Ultraviolet and Isothermal Decomposition of 1,3,5-triamino-2,4,6-trinitrobenzene," *J. Phys. Chem*. **86** 1657-1661 (1982); J. Sharma, J. C. Hoffsommer, D. J. Glover, C. S. Coffey, F. Santiago, A. Stolovy, and S. Tasuda, "Comparative Study of Molecular Fragmentation in Sub-initiated TATB Caused by Impact, UV, Heat and Electron Beams," *In Shock Waves in Condensed Matter—1983*; J. R. Asay, R. A. Graham, and G. K. Straub, eds., Elsevier Science Publisher, 1984; J. Sharma, J. W. Forbes, C. S. Coffey, and T. P. Liddiard, "The Physical and Chemical Nature of the Sensitization Centers left from Hot Spots Caused in Triaminotrinitrobenzene by Shock or Impact, *J. Phys. Chem.* **91**, 5139-5144 (1987); J. Sharma, J. C. Hoffsommer, D. J. Glover, C. S. Coffey, J. W. Forbes, T. P. Liddiard, W. E. Elban, and F. Santiago, "Sub-ignition Reactions at Molecular Levels in Explosives Subjected to Impact and Underwater Shock," *Proceedings of the 8th Detonation Symposium, International*, Office of Naval Research, **MP86-194**, 725-733 (1985).

[11] T. B. Brill and K. J. James, "Kinetics and Mechanisms of Thermal Decomposition of Nitroaromatic Explosives," Wright Laboratory, Armament Directorate report, WL-TR-93-7058, AD-A279 600 (1993); T. B. Brill and K. J. James, "Thermal Decomposition of Energetic Materials. 61. Perfidy in the Amino-2,4,6-Trinitrobenzene Series of Explosives," *J. Phys. Chem.*, **97**, 8752-8758 (1993).

[12] T. A. Land, W. J. Siekhaus, M. F. Foltz, and R. Behrens Jr., "Condensed-Phase Thermal Decomposition of TATB Investigated by Atomic Force Microscopy (AFM) and Simultaneous Thermogravimetric Modulated Beam Mass Spectrometry (STMBMS)," in: *10th Detonation Symposium, International*, Boston, MA, 181-189 (1993).

[13] P. S. Makashir and E. M. Kurian, "Spectroscopic and Thermal Studies on the Decomposition of 1,3,5-triamino-2,4,6-trinitro benzene (TATB)," *J. Thermal Anal*., **46**, 225-236 (1996).

[14] R. Belmas, A. Bry, C. David, L. Gautier, A. Keromnes, D. Poullain, G. Thevenot, C. Le Gallic, J. Chenault, and G. Guillaumet, "Preheating Sensitization of a TATB Composition Part one: Chemical Evolution," *Propellants, Explosives, Pyrotechnics* **29** (5) 282-286 (2004); C. Le Gallic, R. Belmas and P. Lambert, "Preheating Sensitization of a TATB Composition. Part 2: Microstructure Evolution," *Propellants, Explosives, Pyrotechnics* **29** (67) 339-343 (2004); R. Belmas, L. Gautier, C. David, D. Picart, C. Le Gallic, and P. Lambert, "Preheating Sensitization of a TATB Composition Part Three: Sensitization for Various Stimuli. Interpretation and Conclusions," *Propellants, Explosives, Pyrotechnics* **30** (2) 101-104 (2005); D. Poullain, C. David, L. Gautier, and R. Belmas, "Décomposition du TATB," Europyro, Saint-Malo, 23-27, June 2003.

[15] J. A. Carter, J. M. Zaug, A. J. Nelson, M. R. Armstrong, and M. R. Manaa, "Ultrafast Shock Compression and Shock-Induced Decomposition of 1,3,5-Triamino-2,4,6-Trinitrobenzene Subjected to a Subnanosecond-Duration Shock: An Analysis of Decomposition Products," *J. Phys. Chem., A*., **116**, 4851-4859 (2012).